Clays and Clay Minerals, Vol. 60, No. 2, 153–161, 2012.

SORPTION OF NARINGIN FROM AQUEOUS SOLUTION BY MODIFIED CLAY

SOFIA ARELLANO-CARDENAS*, TZAYHRI GALLARDO-VELAZQUEZ, GLORIA V. POUMIAN-GAMBOA, GUILLERMO OSORIO-REVILLA, SOCORRO LOPEZ-CORTEZ, AND YADIRA RIVERA-ESPINOZA

Departamento de Graduados e Investigación en Alimentos, Escuela Nacional de Ciencias Biológicas–IPN, Prol. Plan de Ayala y Carpio, s/n. Col. Santo Tomás, Apartado Postal 42-186, 11340 D.F., México

Abstract—The flavonoid naringin is the main source of the undesirable bitter taste in some citrus juices. In commercial debittering processes, the naringin is adsorbed on non-ionic polymeric resins. Organo-clays (OCs), which have been used as sorbents for organic pollutants, could also have affinity for the naringin molecule, and thus potentially could serve as a debittering agent. The objective of the present study was to characterize the sorption capacity of a prepared OC to evaluate its ability to remove naringin from aqueous solutions, investigating the effect of adsorbent dose, initial concentration of naringin, temperature, contact time, and pH. The OC was prepared by the intercalation of cationic surfactant hexadecyltrimethylammonium bromide in a Mexican bentonite. The host clay and the OC were characterized by X-ray diffraction, Fourier-transform infrared, and nitrogen gas adsorption. The OC showed a surface area of 9.3 $m^2\ g^{-1}$, 11.35 nm average pore diameter, and a basal spacing, d_{001}, of 2.01 nm. The adsorbent removed naringin at the rate of 60−72% at 25ºC and pH 3. The sorption capacity increased with pH and temperature. Experimental data were well fitted by both Langmuir and Freundlich adsorption models. Most of the sorption took place during the first 10 min and the equilibrium time was reached within 720 min. The rate of sorption was adjusted to pseudo second-order kinetics.

Key Words—Adsorbent, Modified Clay, Naringin, Organo-clay, Sorption.

INTRODUCTION

Some processed citrus juices have excessive bitterness that adversely affects the taste and, therefore, the marketability of products made from these juices. The flavonoid naringin is by far the most dominant bitter component in juice of certain orange varieties and in early-season grapefruit (Lee and Kim, 2003). Removal of this sour flavonoid from juice is, therefore, essential for greater consumer acceptance.

Several methods have been developed to remove naringin from aqueous solution: solvent extraction, extraction using supercritical CO_2, ultrafiltration, diafiltration, enzymatic/biological removal, adsorption, and combinations of enzymatic and adsorption techniques (Mishra and Kar, 2003). Adsorption is gaining wider acceptance for large-scale separation from liquids, due to the low-energy nature of the adsorptive separation processes. The different adsorbents reported to reduce the bitterness of citrus juices are: activated carbon, activated florisil, nylon polymers, cyclodextrin polymers, cellulose acetate, and neutral and weak base anion-exchange resins (Singh *et al.*, 2008).

The most widely used adsorbents for industrial applications are non-ionic polymeric resins, which are expensive and the cost of which increases with adsorption capacity. Alternatives are sought. Recently, progress in the synthesis of nanostructured materials has offered new opportunities for assembling functional adsorbents, *e.g.* OCs, which are manufactured from low-cost materials such as clay minerals. The OCs are synthesized by ion exchange of the interlayer cations of expandable layered silicates (*e.g.* montmorillonite) with a large organic cation such as the surfactant hexadecyltrimethylammonium (HDTMA). The properties of these materials change from hydrophilic to hydrophobic, resulting in modified clays with large adsorptive capacities for organic molecules (Anirudhan and Ramachandran, 2006; Erkan *et al.*, 2010). The modified clays are used to remove organic pollutants such as chlorophenols (Yildiz and Gur, 2007), p-nitrophenol (He *et al.*, 2006; Ko *et al.*, 2007), phenol (Arellano-Cárdenas *et al.*, 2008), aniline (Ko *et al.*, 2007), dyes (Juang *et al.*, 2007; Zohra *et al.*, 2008; Jian-min *et al.*, 2010), benzene and toluene (López-Cortez *et al.*, 2008), chlorophenols (Arellano-Cárdenas *et al.*, 2008), tannins (Anirudhan and Ramachandran, 2006; Huang *et al.*, 2008), and petroleum hydrocarbons (Masooleh *et al.*, 2010) from water and vapor phases. The OCs have also been reported as successful adsorbents of mycotoxin in the detoxification of animal feed (Pimpukdee *et al.*, 2004; Wicklein *et al.*, 2008) and in the removal of toxic metals from aqueous solutions (Guerra *et al.*, 2010).

Even though hydrophobic OCs could have affinity for the amphipatic naringin molecule (Figure 1) (Mielczarek, 2005), the sorption of this flavonoid by OCs has not been studied previously. The purpose of the present study was to fill that gap by characterizing the sorption capacity of a prepared OC to evaluate its ability to remove naringin from aqueous solutions. The

* E-mail address of corresponding author:
sarellano@ipn.mx
DOI: 10.1346/CCMN.2012.0600205

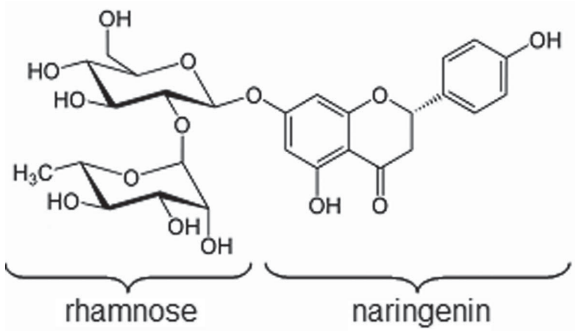

Figure 1. Structure of naringin, 4'5,7-trhihydroxyflavanone 7-rhamnoglucoside. The naringin molecule is a conjugate of a sugar (rhamnose) of hydrophilic nature and the flavanone naringenin of hydrophobic nature (Mielczarec, 2005).

influence of adsorbent dose, initial concentration of naringin, temperature, contact time, and pH on the extent of sorption was also investigated.

MATERIALS AND METHODS

Materials

The clay used in the present study was a Mexican montmorillonite previously characterized by Arellano-Cárdenas *et al.* (2008). The cation exchange capacity (CEC) is 105 meq 100 g^{-1}. This clay was chosen because of its exchange and swelling properties which are suitable for chemical modification, its abundance, and its low cost. The sample was supplied by Arcillas Industriales de Durango, S.A., from northern Mexico. The host clay was crushed and sieved through a stainless steel testing sieve number 65 (mesh size of 0.210 mm), and used without further purification. The surfactant HDTMA $C_{19}H_{42}BrN$ (99.0% pure) and chlorhydrate of naringin $C_{27}H_{32}O_{14}xH_2O$ (minimum 95.0% pure) were purchased from Sigma Aldrich Chemical Co., St. Louis, Missouri, USA.

Preparation of the modified clay

The OC was prepared following a modified version of the method reported by López-Cortez *et al.* (2008). In the present study, the natural clay was mixed with the surfactant HDTMA in an amount equivalent to 100% of its CEC and dissolved in deionized water. This amount of surfactant was used to ensure: (1) that the surfactant mainly occupies the interlayer space in the clay molecules, as reported by He *et al.* (2006); and (2) that the most probable configuration of the interlayered surfactant is as a pseudotrimolecular layer as reported by Nuntiya *et al*. (2008). The system was stirred and allowed to react for 2 h at 50ºC and then for 22 h at 25ºC; the suspension was filtered using a Whatman No. 42 filter paper and was washed repeatedly with deionized water until no bromide anions were detected by 0.1 N $AgNO_3$ solution (K_{sp} AgBr = 5.0×0^{-13}) and the pH of the water was 7. The product was dried at 100ºC for 24 h, ground and sieved through a 0.210 mm mesh, and stored in a desiccator.

Characterization methods

X-ray diffraction (XRD) patterns of clay samples were obtained using a Bruker Model D8 Discover diffractometer, with Ni filter and CuKα radiation (λ = 1.5406 Å). The basal spacing d_{001} was determined using Bragg's equation (Nuntiya *et al.*, 2008; López-Cortez *et al.*, 2008). The Fourier-transform infrared (FTIR) spectra of the host clay and OC were recorded from a KBr disk containing 20 mg of sample and 200 mg of dried KBr, using a Spectrum 2000 spectrophotometer (Houston, Texas, USA). All samples were preheated at 100ºC for 2 h before the measurement (López-Cortez *et al.*, 2008). The surface area of the clay samples was obtained from the N_2/77 K adsorption/desorption isotherms by the BET method (Kaissar *et al.*, 1973) using a Micromeritics ASAP 2020 instrument. The micropore surface was determined by the t-plot method (Dubinin, 1968). The Barrett, Joyner, and Halenda (BJH) method (Barret *et al.*, 1951) was used to evaluate the average pore diameter (He *et al.*, 2006). To determine the point of zero charge (PZC), the potentiometric method was used (Van Raij and Peech, 1971; Arellano *et al.*, 2010). Serial titration curves were made by mixing 0.2 g of OC with 25 mL of aqueous solutions containing (NaCl + HCl) or (NaCl + NaOH) and adjusting the final concentration to 0.1 N. The pH was measured by a Hanna HI 2210 pH-meter (Chula Vista, California, USA). The naringin concentration in aqueous solution was determined using a Thermo Scientific Genesys 10 UV spectrophotometer (Barrington, Madison, Wisconsin, USA) at 280 nm wavelength (Ribeiro *et al.*, 2002).

Batch sorption experiments

The sorption of naringin on the OC was carried out using a batch process (Arellano-Cárdenas *et al.*, 2008). A series of flasks containing 8 g L^{-1} of the OC, 25 mL of the solution of naringin (concentrations ranging from 10 to 900 mg L^{-1}), and citric acid (concentration of 1000 mg L^{-1}) at pH 3 (similar to citric juices) were equilibrated in a temperature-controlled, water-bath shaker for 24 h at 25ºC. Preliminary experiments showed that sorption was completed within 12 h (Figure 2), but to ensure that the equilibrium was attained, a 24 h time period was used. After the equilibrium was reached, the suspensions were filtered through Whatman No. 42 filter paper to remove any remaining adsorbent particles. The filtrates were analyzed for the concentration of residual naringin by spectrophotometry at 280 nm. The sorption experiment was also carried out using the host clay at pH 5 and 25ºC. The clay was separated from the solution after exchange with naringin molecules by centrifugation at $18626 \times g$ using a Hettich MIKRO 200 Microcentrifuge (Ramsey, Minnesota, USA).

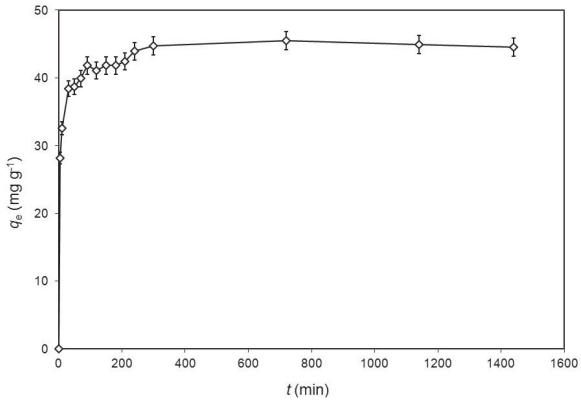

Figure 2. Effect of contact time on naringin sorption on the OC (initial naringin concentration = 500 mg L^{-1}, adsorbent dose = 8 g L^{-1}, T = 25ºC, pH 3).

The specific amount of solute adsorbed was calculated using equation 1 for mass balance:

$$q_e = (C_0 - C_e)\left(\frac{V}{W}\right) \quad (1)$$

where q_e is the sorption capacity of the adsorbent at equilibrium (mg g^{-1}); C_0 and C_e are the initial and equilibrium concentrations of solute, respectively (mg L^{-1}); V is the volume of the aqueous solution (L); and W is the mass of adsorbent used (g).

Effect of temperature. Sorption experiments were also conducted at two additional temperatures, 40 and 60ºC.

Effect of adsorbent dose. Different amounts of adsorbent (4−30 g L^{-1}) were added to 25 mL of naringin solution at an initial concentration of 500 mg L^{-1}, citric acid concentration of 1000 mg L^{-1}, pH 3, and contact time of 24 h at 25ºC.

Kinetics experiments. Kinetics studies were performed using 25 mL of naringin solution with initial concentration of 500 mg L^{-1}, citric acid concentration of 1000 mg L^{-1}, 8 g L^{-1} of the OC, pH 3, and 25ºC, for 24 h. Samples were taken at different time intervals of 5, 10, 20, 30, 40, 50 60, 70, 80, 90, 100, 110, 120, 150, 180, 210, 240, 300, 720, 1140, and 1440 min. Equilibrium was reached at 12 h.

Effect of pH. For pH studies, the sorption experiments were carried out with 8 g L^{-1} of the OC in 25 mL of naringin solution (concentration ranging from 10 to 900 mg L^{-1}) with citric acid (concentration of 1000 mg L^{-1}), at 25ºC for 24 h. The pH of the solutions was adjusted carefully between 2 and 5 using 0.1 N NaOH.

The results reported are the average of triplicate measurements. The error bars shown in the graphs represent the standard deviation values. Statistical significance was defined as p = 0.05.

RESULTS AND DISCUSSION

Characterization of the host clay and the OC

The XRD pattern of the host clay (Figure 3) showed montmorillonite to be the major component of the clay, with traces of quartz, feldspar, and cristobalite. The characteristic first-order reflection peak at 7.06 º2θ gave a d_{001} value of 1.25 nm corresponding to montmorillonite. Also shown is the XRD pattern of the OC with a shift in the first-order reflection to a lower 2θ value (4.4º2θ) compared with the host clay, indicating the expansion of the d_{001} value from 1.25 nm to 2.01 nm. This increase in basal spacing of the modified clay can be attributed to a replacement of the inorganic cations of the host clay by the large cationic surfactant molecules intercalated into the interlayer space of the original clay (Zohra *et al.*, 2008; López-Cortez *et al.*, 2008). This d_{001} value is in agreement with the values reported for HDTMA-montmorillonites (He *et al.*, 2006; Nuntiya *et al.*, 2008). The *d*-spacing values are known to indicate the potential arrangement of interlayer surfactant molecules, which will vary from monolayer (1.37 nm), to bilayer (1.77 nm), to pseudotrimolecular layer (2.17 nm), and to paraffin complexes (>2.2 nm) (He *et al.*, 2006; Nuntiya *et al.*, 2008). The d_{001} value obtained for the OC prepared (2.01 nm) may correspond to the pseudotrimolecular layer model, which is based on the assumption that the surfactant molecules are oriented at right angles to the clay mineral surface (Nuntiya *et al.*, 2008).

The FTIR spectrum of the host clay showed a characteristic profile of montmorillonite (Figure 4). An intense band appeared at 3626 cm^{-1}, due to structural

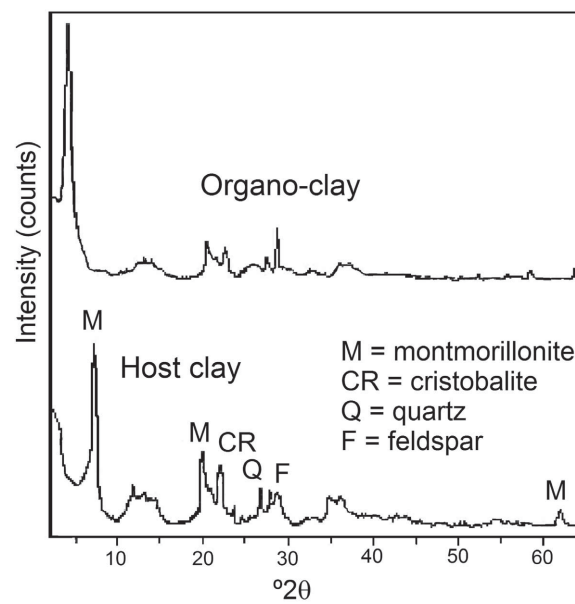

Figure 3. Powder XRD patterns of the host clay and the prepared OC.

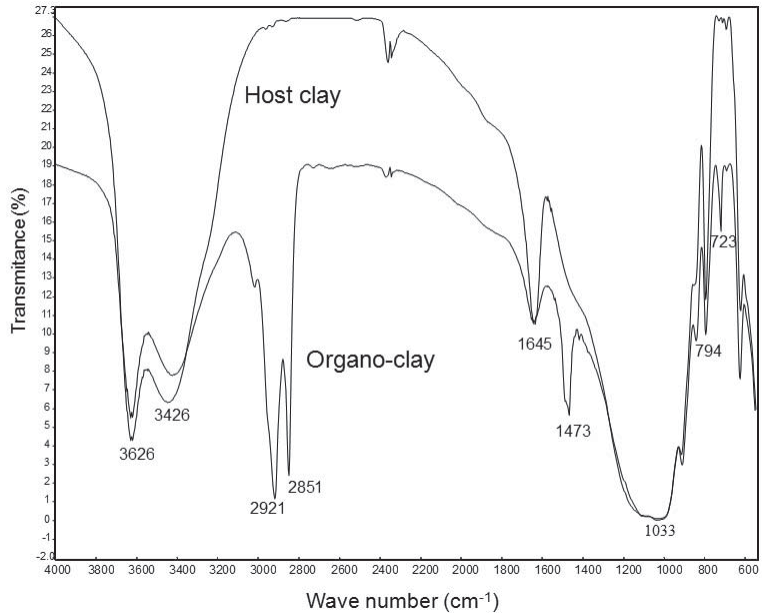

Figure 4. IR spectra of the host clay and of the prepared OC.

O–H stretching, and two other bands at 3426 and 1645 cm^{-1} ascribed to hydrating H_2O molecules. The broad band centered at 1033 cm^{-1} corresponds to the stretching vibration of the Si–O bonds, and the sharp band at 794 cm^{-1} is assigned to silica impurities such as cristobalite (Madejová and Komadel, 2005). The FTIR spectrum of the OC shows the same bands as the host clay but, in addition, strong bands occurred at 2921 and 2851 cm^{-1} and are attributed to asymmetric and symmetric stretching vibrations, respectively, of $-CH_2$ groups of the surfactant hydrocarbon chain (Zohra *et al.*, 2008). A strong absorption peak occurs at 1473 cm^{-1} which can be related to the CH_2 scissoring mode (Othmani-Assmann *et al.*, 2007).

The BET-N_2 specific surface areas (Table 1) were 46.8 and 9.3 $m^2\ g^{-1}$ for the host clay and the OC, respectively. This reduction in the surface area of the OC is attributed to the large intercalated HDTMA cations which could block the pores, thus hindering the passage of N_2 molecules (Juang *et al.*, 2007; He *et al.*, 2006 and, Önal and Sarikaya, 2007). The OC did not exhibit any microporous area (evaluated by the t-plot method) and its average pore diameter obtained by the desorption BJH method (11.3 nm) was larger than in the host clay (8.6 nm) indicating that the clay-modification process may have led to the removal of the original microporous structure existing in the host clay (He *et al.*, 2006; Juang *et al.*, 2007). The surface-area value obtained for the OC (9.3 $m^2\ g^{-1}$) suggested that the surfactant mainly occupies the clay interlayer space. This type of OC was obtained with a surfactant amount of $\leqslant$100% of the CEC of the clay, which has a surface area in the range 9–12 $m^2\ g^{-1}$ (He *et al.*, 2006).

XRD analysis of naringin sorbed on the OC

The XRD spectra of the OC after exchange with naringin molecules (OC-naringin) in the presence of citrate at pH 3 and 5 (Figure 5a, 5b, respectively) showed the same behavior as the original OC (Figure 5c); *i.e.* a d_{001} value between 2.05 and 2.1 nm, indicating that the OC samples retained their surfactant interlayers at these pH values. Citrate anions and naringin molecules did not penetrate into the interlayer space of the OC. The peaks obtained at pH 3 and 5 were less intense and showed greater asymmetry than the original OC, demonstrating that the samples were less crystalline. The adsorbate, therefore, seems to have affected the surfactant arrangement in the interlayer space (Zhou *et al*., 2008).

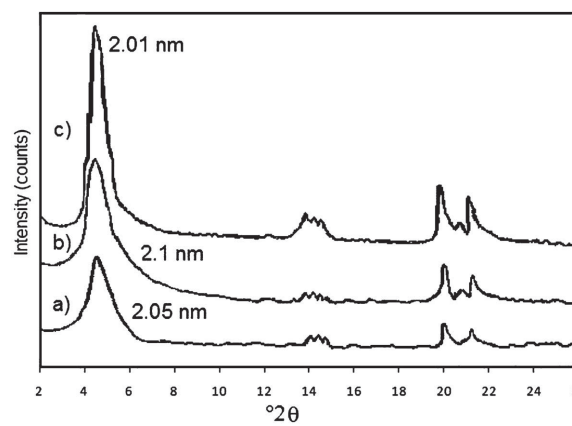

Figure 5. Powder XRD d_{001} reflections of: (c) the OC; and the OC-naringin system in the presence of citric acid at a concentration of 1000 mg L^{-1} at (b) pH 5, (a) pH 3.

In general, the OC showed a stable interlayer in the pH range 3–5, in agreement with the results of Koh *et al.* (2005), who reported no signs of desorption of the organic surfactant of a cetylpyridinium-smectite in the pH range 2–12.

Sorption studies

Effect of adsorbent dose. The percentage of naringin removed increased with increase in OC dose at a fixed solute concentration of 500 mg L^{-1}; while sorption capacity, q_e (amount of naringin sorbed per unit weight of OC), decreased gradually (Figure 6). The percent uptake of solute increased markedly up to an adsorbent dose of 20 g L^{-1} (removal > 90%) and thereafter no significant increase was observed. The increase in percentage of naringin removed was probably due to the increase in number of available sorption sites in accordance with the concentration of the OC (Senturk *et al.*, 2009). The decrease in equilibrium sorption capacity of the OC for naringin uptake can be attributed to the dilution effect due to the increasing amount of OC dose, leaving unsaturated sorption sites on the surface, at constant concentration and volume of the naringin solution. Similar behavior was reported for sorption of tannin onto an organically modified attapulgite clay (Huang *et al.*, 2008) and for sorption of phenol and o-chlorophenol using non-calcined (hydrophobic) MCM-41 silicate material (Mangrulkar *et al.*, 2008).

Effect of solute concentration

The naringin sorption isotherm obtained for the host clay (Figure 7) showed a solute sorption of q_e = 5.5 mg g^{-1} (removal = 1.2%), indicating that this material had no affinity for naringin. This may be due to those cations which balance the permanent surface charge and water, which were preferentially adsorbed by this hydrophilic clay leaving out the large neutral naringin molecules. The OC did, however, show affinity for naringin, and the sorption isotherms obtained at different temperatures display an L-type isotherm according to the Giles *et al.* (1960) classification, indicating that naringin was strongly sorbed on the solid surface and no competition with the solvent for sorption sites was observed. The OC had an affinity for naringin regardless of its smaller surface area (9.3 m^2 g^{-1}) as compared to the host clay (46.3 m^2 g^{-1}); therefore, the distribution and arrangement of the surfactant in the OC were responsible for the sorption efficiency rather than the BET-N_2 surface area. The hydrophobic interaction between organic solutes and OCs is the major mechanism in the sorption process and partitioning often occurs with the smaller-sized solutes (Zhou *et al.*, 2008; Shu *et al.*, 2010). In the present study, considering that naringin molecules have several functional groups (Figure 1), the sorption may involve various types of interactions, *e.g.* hydrophobic interaction between the non-polar parts of the naringin molecules and the alkyl chains of the surfactant, Van der Waals forces, ion-dipole interactions, and hydrogen

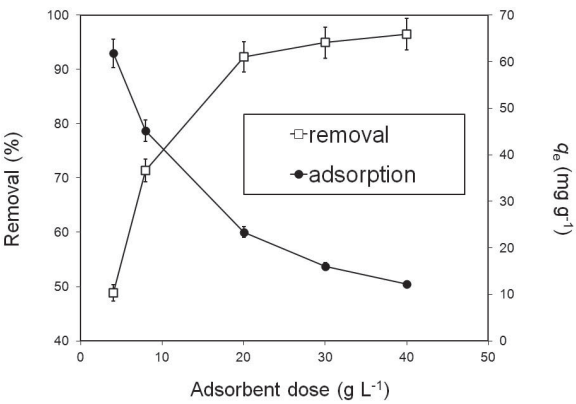

Figure 6. Effect of adsorbent dose on percent removal and naringin sorption (q_e) on the OC (initial naringin concentration = 500 mg L^{-1}, pH 3, T = 25ºC, contact time = 24 h).

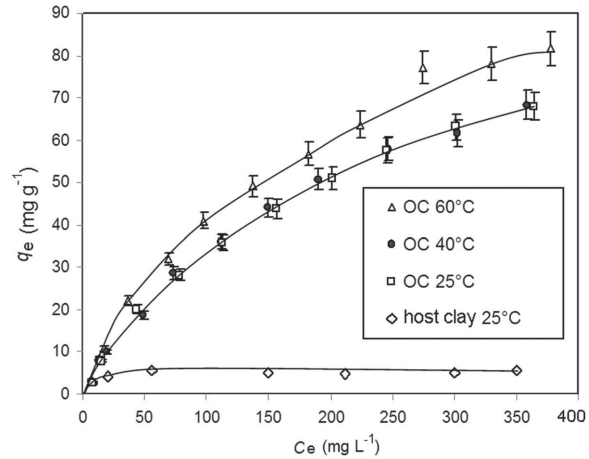

Figure 7. Naringin sorption isotherms on the OC obtained at different temperatures (adsorbent dose = 8 g L^{-1}, pH 3, contact time = 24 h), and on the host clay at pH 5.

Table 1. General properties of the host clay, the OC, and the OC-naringin.

Sample	S_{total} (m^2 g^{-1})	S_{mp} (m^2 g^{-1})	d_p (nm)	ZPC
Host clay	46.8	8.4	8.6	–
OC	9.3	0	11.3	8.0
OC-naringin	4.2	0	8.8	–

S_{total} = specific surface area (evaluated by N_2 isotherm with the BET equation) (Kaissar *et al.*, 1973); S_{mp} = microporous specific area (evaluated by the t-plot method) (Dubinin, 1968); d_p = average pore diameter (evaluated by the desorption BJH method) (Barret *et al.*, 1951). ZPC = zero point of charge (determined by the potentiometric method) (Van Raij and Peech, 1971).

bonding. No partitioning mechanism occurred, however, *i.e.* the large naringin molecule did not intercalate into the interlayer space, as indicated by the XRD analysis (Figure 5). In addition, the BET-N_2 surface area of the OC-naringin decreased 55% compared with the OC (Table 1), indicating that sorption of naringin molecules took place on the external surfaces only.

Effect of temperature

The OC had the same sorption capacity for naringin at 25 and 40ºC (Figure 7), reaching 68 mg g^{-1}, which represents a removal of 60% at pH 3. At 60ºC, the sorption capacity increased slightly to 81.5 mg g^{-1} (removal = 63%) showing that sorption was favored at higher temperatures which is consistent with sorption that involves various kinds of interaction between naringin molecules and the OC. These results agree with those reported for sorption of Direct Red 2 (Zohra *et al.*, 2008), Congo Red (Wang and Wang, 2008), and Crystal Violet (Jian-min *et al.*, 2010) onto HDTMA-montmorillonite.

Sorption models

The data obtained from the sorption of naringin were fitted to the Freundlich and Langmuir adsorption models. The Freundlich isotherm model is valid for heterogeneous adsorbent surfaces with sites that have different energies of adsorption and in the linear form is (Senturk *et al.*, 2009):

$$\log q_e = \log K_F = 1/n \log C_e \quad (2)$$

Where K_F and 1/n are the Freundlich constants related to adsorption capacity and intensity of adsorption, respectively.

The Langmuir model assumes that the adsorption takes place at specific homogeneous sites on the surface of the adsorbent until monolayer formation and the linear form of the Langmuir isotherm model is (Senturk *et al.*, 2009):

$$\frac{C_e}{q_e} = \frac{1}{Q^o b} + \frac{C_e}{Q^o} \quad (3)$$

Where Q^o and b are the Langmuir constants related to a maximum monolayer capacity and energy of adsorption, respectively.

High coefficients of regression (R^2 values range from 0.985 to 0.992) indicate that both models fit the experimental data well (Table 2). For the Freundlich model, 1/n values between 0.67 and 0.71 (<1) represent favorable sorption. For the Langmuir model, the values of Q^o and b increased as temperature increased from 25 to 60ºC, showing that the sorption capacity and intensity were enhanced at higher temperatures. Both models have been reported to reflect well the sorption of aqueous dyes (Zohra *et al.*, 2008); p-nitrophenol, phenol, and aniline (Ko *et al.*, 2007); phenol (Senturk *et al.*, 2009); and p-nitrophenol (Zhu and Chen, 2000; Zhou *et al.*, 2008) by OCs.

Sorption enthalpy

Isosteric heat of adsorption (Q_{st}), defined as the heat of adsorption determined at a constant amount of adsorbate adsorbed, is one of the basic requirements for the characterization and optimization of an adsorption process. The Q_{st} (a positive quantity for exothermic adsorption) is the same as the adsorption enthalpy, ΔH, (a negative quantity for exothermic adsorption) (Domínguez *et al.*, 2010).

The values of ΔH at a different constant surface coverage (q_e) were calculated from the isotherm data measured at 25 and 60ºC (Figure 7) using the Clausius-Clapeyron equation:

$$-\Delta H = Q_{st} = -R\left[\frac{1}{T_2} - \frac{1}{T_1}\right] \ln\left(\frac{C_{e2}}{C_{e1}}\right) \quad (4)$$

where ΔH is the differential adsorption enthalpy (kJ mol^{-1}), Q_{st} is the isosteric heat of adsorption (kJ mol^{-1}), R is the ideal gas constant (8.314 J mol^{-1} K^{-1}), and C_{e1} and C_{e2} are the equilibrium concentrations of the solute (mg L^{-1}) at temperatures T_1 and T_2 (K), respectively.

The plot of ΔH as a function of surface coverage ($\theta = q_e/Q^o$) (Figure 8), where Q^o is the monolayer capacity calculated from the Langmuir equation (Table 2), shows that the heat of sorption increased with increased loading to a maximum value, followed by a decrease. The initial increase in ΔH arose from the dominant adsorbate–adsorbate interactions, and the maximum indicated the energetically heterogeneous surface (adsorbate–adsorbent interactions) (Domínguez *et al.*, 2010).

Table 2. Constants from the Langmuir and Freundlich adsorption models for the sorption of naringin onto the OC.

T (ºC)	Langmuir			Freundlich		
	Q^o (mg g^{-1})	b (L mg^{-1})	R^2	K_F	1/n	R^2
25	104.2	4.9×10^{-3}	0.990	1.16	0.71	0.989
40	104.0	4.4×10^{-3}	0.992	1.43	0.67	0.992
60	120.5	5.45×10^{-3}	0.985	1.60	0.69	0.987

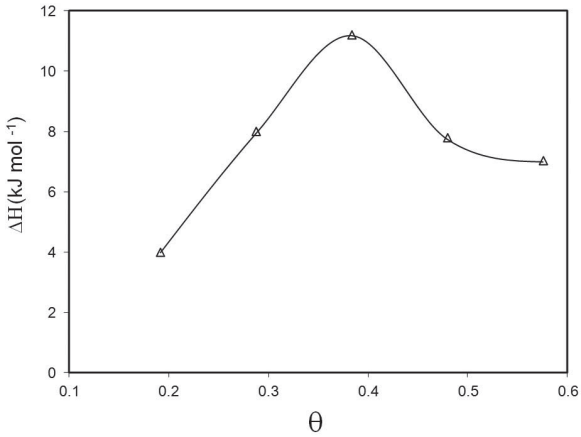

Figure 8. Enthalpy of naringin sorption (ΔH) on the OC as a function of the degree of coverage (θ).

The maximum value obtained for the ΔH was 11.2 kJ mol^{-1} and suggests physisorption because ΔH is <40 kJ mol^{-1}. Furthermore, the positive quantity indicated an endothermic process. These results agree with the physical endothermic adsorption reported for removal of Crystal Violet (Jian-min *et al.*, 2010), Amido Naphthol Red G (Juang *et al.*, 2007), and Direct Red 2 (Zohra *et al.*, 2008) by HDTMA-bentonite.

Kinetics studies

Sorption of naringin by the OC as a function of time at a fixed solute concentration of 500 mg L^{-1} at 25ºC (Figure 2) is the sum of temporal and spatial processes governing sorption onto edges, at interlayer sites, and on external sites. In the initial 'sharp' stage, uptake was rapid – up 32.5 mg g^{-1} (removal = 51%) within the first 10 min. The second was a 'gradual' sorption stage which then stabilized thereafter with no significant removal after 720 min, indicating the attainment of equilibrium at 45.5 mg g^{-1} (removal = 72%). The initial stage indicates rapid attachment of naringin molecules to the external surface of the OC. The second stage is due to diffusion of solute molecules into pores of the adsorbent or other surface reactions. The third step is the final 'equilibrium' stage where internal particle diffusion is very slow due to a low solute concentration in the solution (Mangrulkar *et al.*, 2008; Shu *et al.*, 2010).

In order to investigate the sorption processes of naringin onto the OC, pseudo first- and pseudo second-order kinetics models of sorption were used. These empirical models have been applied widely to a number of aqueous sorption systems (dyes, organics, metal ions) onto different adsorbents (Anirudhan and Ramachandran, 2006; Zohra *et al.*, 2008).

The pseudo first-order (Lagergren) rate equation is related to the kinetics model in which reaction on the surface is the rate-controlling step (Shu *et al.*, 2010; Rudzinski and Plazinski, 2006) (equation 5):

$$\ln(q_e - q_t) = \ln q_e - k_1 t \quad (5)$$

The pseudo second-order model was developed by Ho and Mckay (2000), and is based on the assumption that the chemical sorption is the rate-limiting step. Its linear expression is:

$$\frac{t}{q_t} = \frac{1}{k_2 q_e^2} + \frac{1}{q_e} t \quad (6)$$

where q_t is the amount of solute adsorbed at any time t and q_e is the amount of solute sorbed at equilibrium (mg g^{-1}); k_1 (min^{-1}) and k_2 (g $mg^{-1}min^{-1}$) are the rate constants of the pseudo first-order and the pseudo second-order sorptions, respectively.

The kinetics data obtained gave very good fits with the pseudo second-order model as shown by the R^2 = 0.999 value (Table 3). This model includes all the sorption steps such as external-film diffusion, sorption, and internal particle diffusion (Shu *et al.*, 2010). Several authors have adjusted kinetics data using this pseudo second-order model for studies of sorption of acid and basic dyes (Juang *et al.*, 2007), Direct Red 2 (Zohra *et al.*, 2008), phenol (Senturk *et al.*, 2009), Congo Red (Wang and Wang, 2008), p-nitrophenol (Zhou *et al.*, 2008), chlorobenzenes (Shu *et al.*, 2010), and Crystal Violet (Jian-min *et al.*, 2010) on HDTMA-bentonite.

Effect of pH

The naringin sorption isotherms obtained at different pH values (Figure 9) showed that the isotherms conform to the L-type profile (Giles *et al.*, 1960) and that the amount of naringin sorbed increased with increasing pH. The sorption of naringin increased from 68.5 mg g^{-1} at pH 3, in the presence of citric acid, to a maximum value of 98 mg g^{-1} at pH 5. The pH of the solution is known to affect the degree of ionization and nature of solute and adsorbent which subsequently leads to changes in the equilibrium characteristics of the sorption process (Mangrulkar *et al.*, 2008).

Table 3. Constants from the linear forms of the pseudo first-order and pseudo second-order kinetics models for the sorption of naringin onto the OC.

Pseudo first-order model			Pseudo second-order model		
k_1 (min^{-1})	q_e (mg g^{-1})	R^2	k_2 (g $mg^{-1}min^{-1}$)	q_e (mg g^{-1})	R^2
0.0047	14.68	0.724	0.0128	50.50	0.999

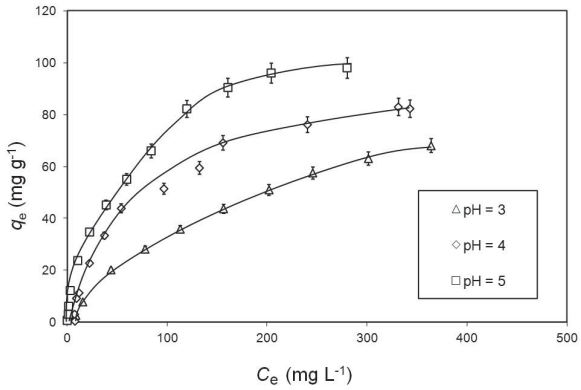

Figure 9. Effect of pH on naringin sorption on the OC (T = 25ºC, adsorbent dose = 8 g L^{-1}, citric acid concentration = 1000 mg L^{-1}, contact time = 24 h).

The naringin molecule is stable in aqueous solution within the pH range 1−11 and its dissociation constants are pK_1 = 9.0 and pK_2 = 9.91 (Mielczarek, 2005). Citric acid has three COOH functional groups with pK_1 = 3.15, pK_2 = 4.76, and pK_3 = 6.40 (Singh *et al.*, 1996). Therefore, in the pH range 3−5, the non-dissociated (neutral) form of naringin and the citrate ion prevailed. On the other hand, the PZC determined for the OC was 8 (Table 1) so the OC surface carries a positive charge at these pH values of 3−5. Citrate ions can be sorbed onto the surface of the OC in competition with the naringin molecules. As the pH was increased, the positive surface charge of the OC decreased resulting in less sorption of citrate and greater sorption of naringin. Citrate sorbs very weakly to both illite and kaolinite, with maximum sorption between pH 4.5 and 7 (Lackovic *et al.*, 2003), and sorption of citrate onto kaolinite was greater at pH 4 than at pH 6 or 8 (Singh *et al.*, 1996). Those authors suggested that adsorption of citrate occurred on the surface hydroxyl groups only.

CONCLUSIONS

The organo-clay obtained in the present study was characterized using XRD, FTIR, and BET-N_2 analysis. The OC prepared showed a good sorption capacity for removal of the flavonoid naringin from aqueous solution. The sorption of naringin was pH dependent. Langmuir and Freundlich sorption models both predicted accurately the sorption in the temperature range 25−60ºC. The sorption kinetics data were well described using the pseudo second-order kinetics model. Physisorption appeared to be the dominant process in the sorption of naringin onto the OC.

The OC prepared here represents a potential sorbent for the sorption of the naringin present in aqueous media. Further studies are required to test removal from real citrus juice.

ACKNOWLEDGMENTS

Financial support from the Secretaría de Estudios de Posgrado e Investigación del Instituto Politécnico Nacional de México (SIP-IPN) and the Consejo Nacional de Ciencia y Tecnología (CONACYT) is appreciated.

The authors are indebted to Dr Jesús Palacios Gómez of the Department of Materials Science (ESFM-IPN) for assistance with the XRD analysis.

REFERENCES

Anirudhan, T.S. and Ramachandran, M.J. (2006) Adsorptive removal of tannin from aqueous solutions by cationic surfactan-modified bentonite clay. *Colloid and Interface Science*, **299**, 116−124.

Arellano, C.S., Gallardo, V.T. Osorio, R.G., and López, C.S. (2010) Study of the surface charge of a Porous Clay Hetersostructure (PCH) and its adsorption capacity of alkaline metal. *Journal of the Mexican Chemical Society*, **54**, 92−97.

Arellano-Cárdenas, S., Gallardo-Velázquez, T., López-Cortez, S., and Osorio-Revilla, G. (2008) Preparation of a Porous Clay Heterostructure (PCH) and study of its adsorption capacity of phenol and chlorinated phenols from aqueous solutions. *Water Environment Research*, **80**, 60−67.

Barret, E.P., Joyner, L.G. and Halenda, P.P. (1951) The determination of pore volume and area distributions in porous substances 1. Computations from nitrogen isotherms. *Journal of Colloid and Interface Science*, **73**, 373-380.

Domínguez, G., Hernández, H.R., and Aguilar, A.G. (2010) Isosteric heats of adsorption of N_2O and NO on natural zeolites. *Journal of Mexican Chemical Society*, **54**, 111−116.

Dubinin, M.M. (1968) Porous structure of adsorbents and catalysts. *Advances in Colloid and Interface Science*, **2**, 217−235.

Erkan, L., Alp, B., and Celik, M.S. (2010) Characterization of organo-bentonites obtained from different linear-chain quaternary alkylammmonium salts. *Clays and Clay Minerals*, **58**, 792−802.

Giles, C.H., MacEwan, T.H., Nakwa, S.N., and Smith, D. (1960) Studies in adsorption. Part. XI. A system of classification of solution adsorption isotherms, and its use in diagnosis of adsorption mechanisms and in measurement of specific surface areas of solids. *Journal of the Chemical Society*, **3**, 3973−3993.

Guerra, D.L., Ferreira, J.N., Pereira, M.J., Viana, R.R., and Airoldi, C. (2010) Use of natural and modified magadiite as adsorbents to remove Th(IV), U(VI), and Eu(III) from aqueous media − thermodynamic and equilibrium study. *Clays and Clay Minerals*, **58**, 327−339.

Kaissar, M. H., Odler, I., Brunauer, S., Hagymassy J. Jr, and Bodor, E.E. (1973) Pore structure analysis by oxygen adsorption. II. Analysis of five silica gels. *Journal of Colloid and Interface Science*, **45**, 38−54.

He, H., Zhou, Q., Martens, W.N., Kloprogge, T.J., Yuan, P., Xi, Y., Zhu, J., and Frost, R.L.M. (2006) Microstructure of HDTMA-modified montmorillonite and its influence on sorption characteristics. *Clays and Clay Minerals*, **54**, 689−695.

Ho, H.S. and McKay, G. (2000) The kinetics of sorption of divalent metal ions onto Sphagnum moss peat. *Water Research*, **34**, 735−742.

Huang, J.H., Liu, Y., and Wang, W. (2008) Selective adsorption of tannin from flavonoids by organically modified attapulgite clay. *Journal of Hazardous Materials*, **160**, 382−387.

Jian-min, R., Si-wei, W., and Wei, J. (2010) Adsorption of

crystal violet onto BTEA- and CTMA-bentonite from aqueous solutions. *World Academy of Science, Engineering and Technology*, **65**, 790−795.

Juang, L., Wang, C., Lee, C., and Hsu, T. (2007) Dyes adsorption onto organoclay and MCM-41. *Journal of Environmental Engineering, Management*, **17**, 29−38.

Ko, C.H., Fan, C., Chiang, P.N., Wang, M.K., and Lin, K.C. (2007) *p*-Nitrophenol, phenol and aniline sorption by organo-clays. *Journal of Hazardous Materials*, **149**, 275−282.

Koh, S.M., Song, M.S., and Takagi, T. (2005) Mineralogy, chemical characteristics and stabilities of cetylpyridinium-exchanged smectite. *Clay Minerals*, **40**, 213−222.

Lackovic, K., Johonson, B.B., Angove, M.J., and Wells, J.D. (2003) Modeling the adsorption of citric acid onto Muloorina illite and related clay minerals. *Journal of Colloid and Interface Science*, **267**, 49−59.

Lee, H.S. and Kim, J.G. (2003) Effects of debittering on red grapefruit juice concentrate. *Food Chemistry*, **82**, 177−180.

López-Cortez, C., Osorio-Revilla, G., Gallardo-Velázquez, T., and Arellano-Cárdenas, S. (2008) Adsorption of vapor-phase VOC's (benzene and toluene) on modified clays and its relation with surface properties. *Canadian Journal of Chemistry*, **86**, 305−311.

Madejová, J. and Komadel, P. (2005) Information available from infrared spectra of the fine fractions of bentonites. Pp. 65−98 in: *The Application of Vibrational Spectroscopy to Clay Minerals and Layered Double Hydroxides* (J.T. Kloprogge, editor). CMS Workshop Lectures, Vol. **13**. The Clay Minerals Society, Aurora, Colorado, USA.

Mangrulkar, P.A., Kamble, S.P., Meshram, J., and Rayalu, S.S. (2008) Adsorption of phenol and o-chlorophenol by mesoporous MCM-41. *Journal of Hazardous Materials*, **160**, 414−421.

Masooleh, M.S., Bazgir, S., Tamizifar, M., and Nemati, A. (2010) Adsorption of petroleum hydrocarbons on organo-clay. *Journal of Applied Chemical Researches*, **4**, 19−23.

Mielczarek, C. (2005) Acid-base properties of selected flavonoid glycosides. *European Journal of Pharmaceutical Sciences*, **25**, 273−279.

Mishra, P. and Kar, R. (2003) Treatment of grapefruite juice for bitterness removal by Amberlite IR 120 and Amberlite IR 400 and alginate entrapped nainginase enzyme. *Journal of Food Science*, **68**, 1229−1233.

Nuntiya, A., Sompech, S., Aukkaravittayapun, S., and Pumchusak, J. (2008) The effect of surfactant concentration on the interlayer structure of organoclay. *Chiang Mai Journal of Science*, **35**, 199−205.

Önal, M. and Sarikaya, Y. (2007) Some physicochemical properties of partition nanophases formed in sorptive organoclays. *Colloids and Surfaces A: Physicochemical Engineering Aspects*, **296**, 216−221.

Othmani-Assmann, H., Benna-Zayani, M., Geiger, S., Fraisse, B., Kbir-Ariguib, N., Trabelsi-Ayadi, M., Ghermani, N.E., and Grossiord, J.L. (2007) Physico-chemical characterizations of Tunisian organophilic bentonites. *Journal of Physical Chemistry*, **111**, 10869−10877.

Pimpukdee, K., Tengjaroenkul, B., Chaveerachl, P., and Mhosatanun, B. (2004) Characterization of clays and cetylpiridinium-exchanged clays for their ability to adsorb Zearalenone. *Thai Journal of Veterinary Medicine*, **34**, 24−31.

Ribeiro, M.H.L., Silveira, D., and Ferreira, D.S. (2002) Selective adsorption of limonin and naringin from orange juice of naural and synthetic adsorbents. *European Food Research Technology*, **215**, 462−471.

Rudzinski, W. and Plazinski, W. (2006) Kinetics of solute adsorption at solid/solution interfaces: A theoretical development of the empirical pseudo-first and pseudo-second order kinetic rate equations, based on applying the statistical rate theory of interfacial transport. *Journal of Physical Chemistry, B*, **110**, 16514−16525.

Senturk, H.B., Ozdes, D., Gundogdu, A., Duran, C., and Soylak, M. (2009) Removal of phenol from aqueous solutions by adsorption onto organomodified Tirebolu bentonite: equilibrium, kinetic and thermodynamic study. *Journal of Hazardous Materials*, **172**, 353−362.

Shu, Y., Li, L., Zhang, Q., and Wu, H. (2010) Equilibrium, kinetics and thermodynamic studies for sorption of chlorobenzenes on CTMAB modified bentonite and kaolinite. *Journal of Hazardous Materials*, **173**, 47−53.

Singh, J., Huangh, P.M., Hammer, U.T., and Liaw, W.K. (1996) Influence of citric acid and glycine on the adsorption of mercury (ii) by kaolinite under various pH conditions. *Clays and Clay Minerals*, **44**, 41−48.

Singh, S.V., Gupta, A.K., and Jain, R.K. (2008) Adsorption of naringin on nonionic (neutral) macroporous adsorbent resin from its aqueous solution. *Journal of Food Engineering*, **86**, 259−271.

Van Raij, B. and Peech, M. (1971) Electrochemical properties of some oxisols and alfisols of the tropics. *Soil Science Society of America*, **36**, 587−593.

Wang, L. and Wang, A. (2008) Adsorption properties of Congo Red from aqueous solution onto surfactant-modified montmorillonite. *Journal of Hazardous Materials*, **160**, 173−180.

Wicklein, B., Darder, M., Aranda, P., and Ruiz-Hitzky, E. (2008) Organically modified clays for uptake of mycotoxins. *Revista de la Sociedad Española de Mineralogía*, **9**, 257−258.

Yildiz, A. and Gür, A. (2007) Adsorption of phenol and chlorophenols on pure and modified sepiolite. *Journal of the Serbian Chemistry Society*, **72**, 467−474.

Zhou, Q., He, H.P., Zhu, J.X., Shen, W., Frost, R.L., and Yuan, P. (2008) Mechanims of *p*-nitrophenol adsorption from aqueous solution by $HDTMA^+$-pillared montmorillonite-Implications for water purification. *Journal of Hazardous Materials*, **154**, 1025−1032.

Zhu, L. and Chen, B. (2000) Sorption behavior of p-Nitrophenol on the interface between anion-cation organobentonite and water. *Environmental Science & Technology*, **34**, 2997−3002.

Zohra, B., Aicha, K., Fatima, K.S., Nourredine, B., and Zoubir, D. (2008) Adsorption of Direct Red 2 on bentonite modified by cetyltrimethylammonium bromide. *Chemical Engineering Journal*, **136**, 295−305.

(*Received 28 April 2011; revised 20 March 2012; Ms. 566; A.E. S. Petit*)